American Mineralogist, Volume 97, pages 1905–1914, 2012

The atomic structure of deuterated boyleite $ZnSO_4 \cdot 4D_2O$, ilesite $MnSO_4 \cdot 4D_2O$, and bianchite $ZnSO_4 \cdot 6D_2O$

Jennifer L. Anderson,[1] Ronald C. Peterson,[1,*] and Ian Swainson[2,†]

[1]Department of Geological Sciences and Geological Engineering, Queen's University Kingston, Ontario K7L 3N6, Canada
[2]Canadian Neutron Beam Center, National Research Council, Chalk River Laboratories, Chalk River, Ontario, K0J 1J0, Canada

Abstract

Deuterated boyleite $ZnSO_4 \cdot 4D_2O$, was synthesized and the atomic structure, including D positions, was successfully refined in a combined histogram neutron diffraction refinement. The cell dimensions for boyleite are a = 5.9144(2), b = 13.5665(4), c = 7.8924(2) Å, and β = 90.668(2)° with space group $P2_1/n$ and Z = 4. The atomic structure including D positions of the isostructural mineral ilesite, $MnSO_4 \cdot 4D_2O$, was refined and the cell dimensions are a = 5.9753(1), b = 13.8186(3), c = 8.0461(1) Å, and β = 90.826(2)°. Deuterated bianchite $ZnSO_4 \cdot 6D_2O$ was synthesized and the atomic structure, including D positions, was successfully refined with a unit cell of a = 9.969(1), b = 7. 2441(7), c = 24.249(3) Å, and β = 98.488(5)° in space group $C2/c$ and Z = 8. A comparison of the hydrogen bonding in $M^{2+}SO_4 \cdot 4D_2O$ with that in $M^{2+}SO_4 \cdot 6D_2O$ shows that bifurcated hydrogen bonds are common in the tetrahydrate sulfates but nonexistent in the hexahydrate structures. This is a result of the packing constraints of the rings of the sulfate and metal-containing octahedra in the tetrahydrates. In the hexahydrate sulfates there is no direct linkage between the sulfate and metal-containing octahedra and hydrogen bonds are optimized without packing constraints, and no bifurcated hydrogen bonds are observed.

Keywords: Bianchite, boyleite, ilesite, hexahydrite, moorhouseite, Ni-hexahydrite, rozenite, crystal-structure refinement, neutron diffraction, hydrogen bonding

Introduction

The minerals boyleite, $ZnSO_4 \cdot 4H_2O$, and ilesite, $MnSO_4 \cdot 4H_2O$, are members of the rozenite group ($M^{2+}SO_4 \cdot 4H_2O$; M^{2+} = Fe, Mg, Mn, Co, Zn) $P2_1/n$ (Table 1) (Gaines et al. 1997). All rozenite group minerals structures are composed of isolated $[M^{2+}(SO_4)]_2 \cdot 8H_2O$ ring-shaped structural units (Fig. 1), linked to each other by a three-dimensional network of H-bonds.

Boyleite was first described by Walenta (1978) as a product of sphalerite decomposition in the presence of gypsum. The type specimen of boyleite has a chemical composition of $(Zn_{0.84}Mg_{0.16})SO_4 \cdot 4H_2O$ and was found as white, earthy, reniform masses at the Kropback quarry, southern Black Forest, Germany (Walenta 1978). More recently described occurrences of boyleite include the Mole River mine, northern New South Wales (Ashley and Lottermoser 1999), and Valais, Switzerland (Perroud et al. 1987). The presence of boyleite is dependent on the dehydration rate; therefore, boyleite may be present in many localities where goslarite $ZnSO_4 \cdot 7H_2O$, bianchite $ZnSO_4 \cdot 6H_2O$, and gunningite $ZnSO_4 \cdot H_2O$ are found. Notable hydrous Zn-sulfate mineral localities include the type locality of gunningite, Keno Hill-Galena Hill area, Yukon, (Jambor and Boyle 1962) and the Geul Valley goslarite locality near Moresnet, Belgium (Schuiling 1992). Ilesite was first described in 1881 by Iles as an alteration product of sulfide veins at the head of the Hall Valley, Park County, Colorado. The optical properties of synthetic material were described by Larsen and Glenn (1920).

The atomic structure of boyleite was determined by X-ray diffraction analysis of a single crystal produced as an unexpected by-product of another experiment (Blake et al. 2001, annotated by Baur 2002). The use of X-rays to determine H-positions, whose bond lengths were then restrained, and the hydration/dehydration of the sample during data collection, which was partially corrected with a linear isotropic crystal decay correction factor, contributed to the compromised quality of the boyleite data set (Blake et al. 2001). Baur (2002) predicted that the structure of ilesite is very similar to that of rozenite and the atomic structure and approximate hydrogen positions of ilesite were confirmed by Held and Bohaty (2002) through the least-squares refinement of single-crystal X-ray diffraction data.

Bianchite is a member of the hexahydrite group group ($M^{2+}SO_4 \cdot 4H_2O$; M^{2+} = Fe, Mg, Mn, Co, Zn, Ni) $C2/c$ (Table 1) (Gaines et al. 1997). All hexahydrite group minerals structures are composed of isolated $[M^{2+}(H_2O)_6]$ octahedra and sulfate tetrahedra held together only by hydrogen bonding. Minerals of the hexahydrite group are commonly associated with metal sulfide minerals that have been exposed to hydration and oxidation processes. Natural occurrences of the hexahydrite group of minerals indicate that these minerals are often intermixed with

* E-mail: peterson@geol.queensu.ca
† Present address: Canadian Centre for Nuclear Innovation, 111-105 North Road (Peterson Building), Saskatoon S7N 4L5, Canada.

0003-004X/12/1112–1905$05.00/DOI: http://dx.doi.org/10.2138/am.2012.4121

TABLE 1. Unit-cell dimensions for rozenite group minerals $P2_1/n$ and hexahydrite group minerals $C2/c$

M^{2+}	Mineral	a (Å)	b (Å)	c (Å)	β (°)	V (Å^3)	Reference
Mg	starkeyite	5.922(6)	13.604(4)	7.905(5)	90.85(17)	636.8	Baur (1962)
Mg	starkeyite	5.922(6)	13.604(4)	7.905(5)	90.85(17)	636.8	Baur (1964a)
Co	aplowite	5.952(1)	13.576(2)	7.908(1)	90.53(1)	638.9	Kellersohn (1992)
Co	aplowite	5.94	13.56	7.90	90.5	634.3	Jambor and Boyle (1965)
Fe	rozenite	5.979(4)	13.648(4)	7.977(3)	90.4(2)	650.1	Baur (1962)
Fe	rozenite	5.94	13.59	7.94	90.5	641.5	Jambor and Traill (1963)
Zn	boyleite	5.904(3)	13.519(6)	7.883(6)	90.26(6)	629.2	Blake et al. (2001)
Zn	boyleite	5.9144(2)	13.5665(4)	7.8924(2)	90.668(2)	633.2	boyleite, this study
Mn	ilesite	5.9783(6)	13.809(1)	8.0481(7)	90.80(1)	664.3	Held and Bohaty(2002)
Mn	ilesite	5.9753(1)	13.8186(3)	8.0461(1)	90.826(2)	664.3	ilesite, this study
Mg	hexahydrite	10.110(5)	7.212(4)	24.410(1)	98.30(5)	1761.2	Zalkin et al. 1964
Zn	bianchite	9.969(1)	7.2441(7)	24.249(3)	98.488(5)	1732.0	bianchite, this study
Fe	ferrohexahydrite	10.08	7.28	24.59	98.37	1785.3	Vlasov and Kuznetsov (1962)
Ni	nickel-hexahydrite	9.878(2)	7.214(2)	24.065(6)	98.37(2)	1696.6	Gerkin and Reppart (1988)
Co	moorehouseite	10.022(3)	7.217(2)	24.224(3)	98.42(2)	1733.2	Elerman (1988)
Mn	chvaleticeite	10.05(2)	7.24(2)	24.3(1)	98.0(2)	1750.9	Pasava et al. (1986)

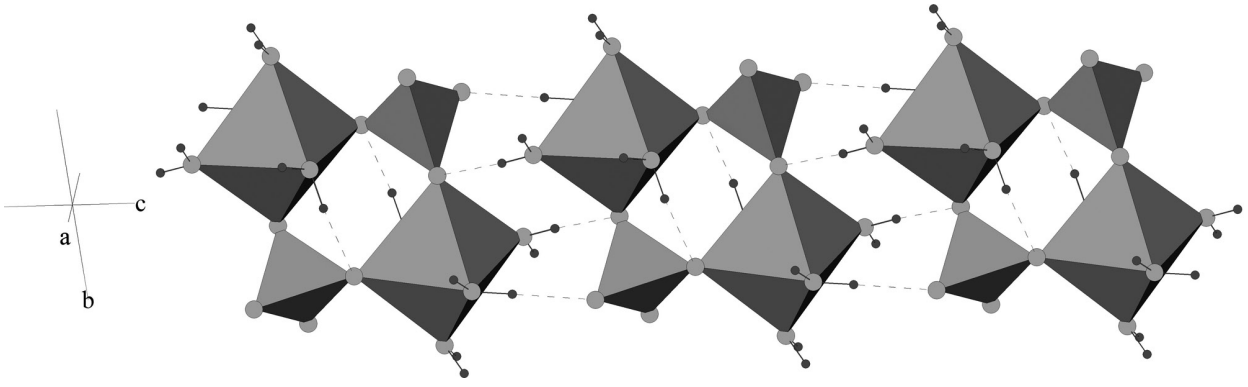

FIGURE 1. Three four-membered $[Zn^{2+}(SO_4)]_2 \cdot 8H_2O$ rings in boyleite consisting of two sulfate tetrahedra and two zinc-containing octahedra sharing corners. The four D_2O molecules form part of the coordination of zinc. Deuterium atoms are shown as small spheres (Dowty 2011). Hydrogen bonding links these groups together.

minerals of the epsomite and/or kieserite group minerals. The hydration and dehydration behavior of these minerals is complex and varies with temperature, relative humidity, acidity, chemical composition as well as the rate of change of these parameters. Bianchite has been observed by the authors at the Baccu Locci Mine, Sardinia (Bakos et al. 1990), and the Brunswick Mine, Bathurst, New Brunswick, Canada, where it is closely associated with goslarite, boyleite, and gunningite.

The atomic structures and hydrogen positions have been determined for some of the iso-structural members of the hexahydrite group minerals or their synthetic equivalents (Zalkin et al. 1964; Kellersohn et al. 1993a; Bargouth and Will 1981; Batsanov 2000) but not for bianchite, chvaleticeite $MnSO_4 \cdot 6H_2O$ and ferrohexahydrite $FeSO_4 \cdot 6H_2O$. Chvaleticeite and ferro-hexahydrite are not commonly observed in nature.

The present study presents the refined atomic structures, including D positions, of boyleite, ilesite, and bianchite as determined by the refinement of neutron diffraction data collected from synthetic, deuterated powder specimens.

PHASE RELATIONSHIPS

Figure 2 presents the phase diagram for the $ZnSO_4 \cdot H_2O$ system showing the fields of stability for goslarite and bianchite as determined by the humidity-buffer method (Chou and Seal 2005) and the position of the bianchite-gunningite boundary based on thermodynamic data (Wagman et al. 1982). A field of stability for boyleite is not represented in the diagram. Similarly the tetrahydrate, starkeyite, of the $MgSO_4 \cdot H_2O$ system, is absent from the relevant equilibrium phase equilibria diagram of Chou et al. (2005) and has been found to be metastable based on thermodynamic data (Grevel and Majzlan 2009). The derived standard Gibbs free energy of reaction for the hexahydrite-starkeyite transformation has been determined by the humidity buffer method (Chou et al. 2005). In thermo-gravimetric experiments in the $ZnSO_4 \cdot H_2O$ system boyleite may or may not be observed and this behavior is likely due to differences in the heating rate and sample history (Guenot et al. 1969; Pannetier et al. 1966; Uvaliev and Motornaya 1989). The appearance of aplowite $CoSO_4 \cdot 4H_2O$ during the dehydration of synthetic bieberite $CoSO_4 \cdot 7H_2O$ (Sinha and Deshpande 1989) and the appearance of boyleite during the dehydration of bianchite is suggested to be dependent on the history of the sample although the difficulty in detecting these phases in thermo-gravimetric dehydration experiments may be due to the narrow field of stability of these minerals (Guenot et al. 1969). Rhomer (1939) reports that in the $MnSO_4 \cdot H_2O$ system, ilesite $MnSO_4 \cdot 4H_2O$ does not occur as a stable phase during the dehydration of synthetic mallardite $MnSO_4 \cdot 7H_2O$. Rozenite $FeSO_4 \cdot 4H_2O$ is the only rozenite group mineral observed to have a well-defined field of stability (Chou et al. 2002). The differing dehydration paths observed for these materials may be the result

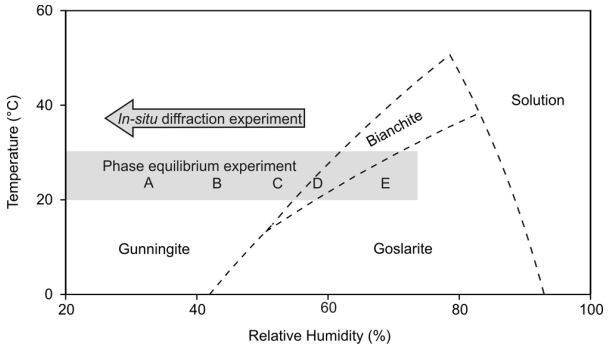

FIGURE 2. The equilibrium phase diagram for the $ZnSO_4 \cdot H_2O$ system. The dashed lines are reproduced from Chou and Seal (2005) and references therein. Symbols A through E indicate the conditions of the glove-box relative-humidity chamber dehydration experiments. At A (33% RH) goslarite dehydrated to boyleite and remained a single phase for 11 days before dehydrating to gunningite. At B (43% RH) goslarite dehydrated to boyleite and remained a single phase for 70 days before dehydrating to gunningite. At C (54% RH) goslarite dehydrated to bianchite; at D (59% RH) a mixture of goslarite and bianchite remained in the sample after one year; and at E (69% RH) goslarite remained after one year. The arrow represents conditions of the in situ diffraction experiment (57–26% RH, 37 °C) where goslarite dehydrated rapidly to a mixture of bianchite, boyleite, and gunningite and shown in Figure 3.

of kinetic limitations on the various dehydration reactions. The dehydration of goslarite to boyleite appears to be more favored than dehydration to bianchite under conditions sufficiently far from equilibrium conditions. Figure 2 presents the results of five static experiments where goslarite powder was left to equilibrate for up to a year under controlled relative humidity conditions. The results are consistent with the phase boundary of Chou and Seal (2005). Also shown in Figure 2 is the range of humidity at 37 °C under which in situ measurements were made of the stability of goslarite using a chamber described by Peterson and Grant (2005). A small amount of finely ground goslarite was dusted onto a glass plate. The chamber was closed and the temperature of the sample reached 37 °C within 2 min. The humidity was 39% when the chamber was closed and increased to 57% after 25 min. An X-ray diffraction scan at this time showed that the amount of goslarite had decreased and bianchite had begun to form but there was no evidence of boyleite or gunningite. After 85 min the humidity was 42% and bianchite had continued to grow at the expense of goslarite and boyleite and gunningite had yet to appear. At 130 min with a relative humidity of 26%, bianchite reached the maximum amount that was generated and some boyleite and a significant amount of gunningite had formed. At 150 min with a relative humidity of 26%, a small amount of goslarite and bianchite remained with a slight increase in boyleite but the sample was mostly gunningite based on relative intensities of the X-ray diffraction peaks. Figure 3 shows the results of these in situ experiments. This non-equilibrium experiment was conducted under the temperature and relative humidity conditions where gunningite is the predicted stable phase (Fig. 2). The order of appearance of the bianchite, boyleite, and gunningite is consistent with a process where the dehydration reaction is controlled by diffusion of H_2O. The initial sample of goslarite was finely ground but the formation of the lower hydrates is controlled by the diffusion of H_2O from these fine grains. Over time the grains become zoned with the lower hydrates forming on the outside and limiting further diffusion of H_2O from the higher hydrate phases remaining in the center of the grains.

SYNTHESIS

Boyleite

Deuterated crystals of goslarite were synthesized from solution using a mixture of reagent grade $ZnSO_4 \cdot 7H_2O$ (Fisher Z68) and 0.1 M D_2SO_4 [prepared from D_2O (AECL ZX098) and D_2SO_4 (C/D/N Isotopes Inc. D-39)] (Anderson et al. 2005). The deuterated goslarite was synthesized, dissolved in 0.1 M D_2SO_4 and the synthesis was repeated until the infrared spectrum of goslarite showed a maximum D_2O:H_2O peak height ratio. The well-deuterated goslarite was powdered and placed in a chamber of 43% relative humidity at 23 °C, buffered by a saturated salt solution of $MgNO_3$-D_2O (Greenspan 1977) and left for 10 days to produce the deuterated boyleite used in the neutron diffraction experiment. This synthesized boyleite was powdered within the buffered-humidity environment to prevent any hydration, dehydration, or H-D exchange of the sample. Prior to removal from the humidity-buffered chamber the sample was sealed inside the vanadium sample canister used for the neutron diffraction experiment to prevent H-D exchange or dehydration.

The infrared spectrum of boyleite (Fig. 4) was obtained with a Nicolet Avatar 320 Fourier-transform infrared spectrometer and a Golden Gate diamond ATR. Comparison of the boyleite spectra with that of liquid water shows there to be very little hydrogen in the sample studied.

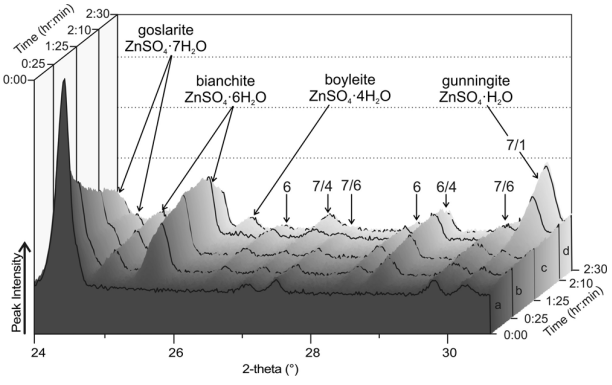

FIGURE 3. Results of the in situ diffraction experiment in a relative humidity and temperature controlled chamber (Peterson and Grant 2005). A sample of finely ground goslarite (indicated as 7) was dusted onto a low-background sample holder and placed into the chamber at 37 °C. (**a**) The initial scan (t = 0:00) shows a single phase of goslarite and subsequent histograms show the dehydration of goslarite and the growth of bianchite (6). (**b**) Bianchite growth continues as boyleite (4) and gunningite (1) peaks emerge. (**c**) Gunningite grows at the expense of goslarite and bianchite. The relative humidity in the chamber was lowered from 57 to 26% relative humidity at 37 °C during the course of the 2.5 h long experiment.

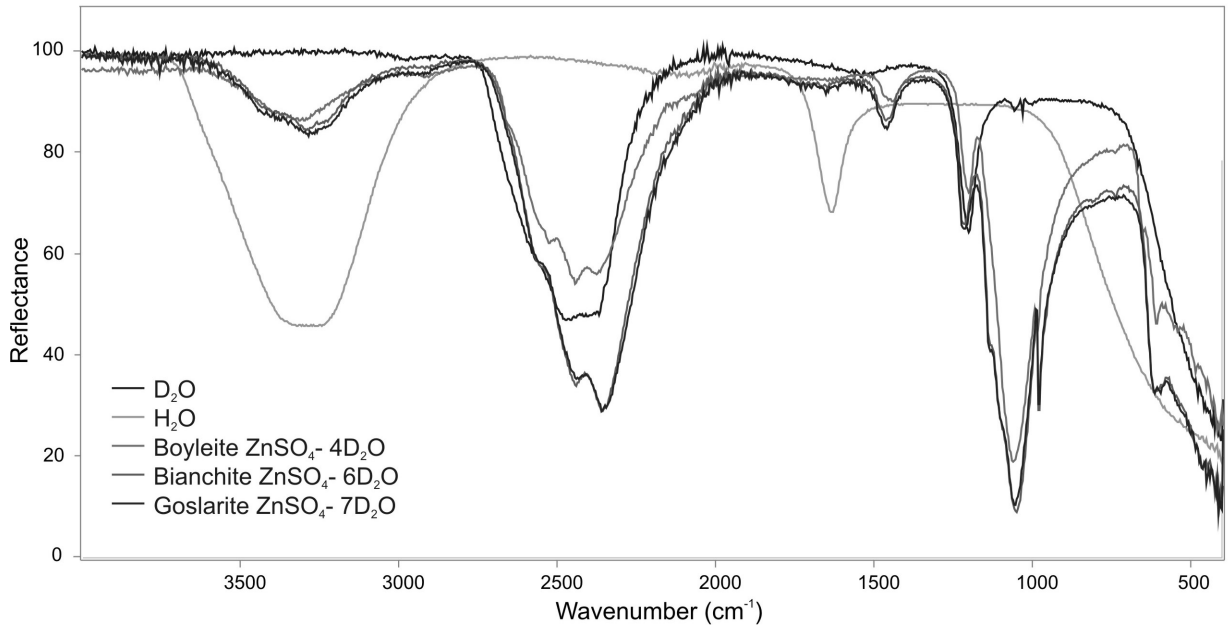

FIGURE 4. Infrared reflectance spectra of deuterated samples of boyleite, bianchite, and goslarite.

Ilesite

Ilesite was synthesized through precipitation directly from a solution of $MnSO_4$ (AC42391-5000) and 0.1 M D_2SO_4 at 23 °C. This was accomplished within a glove box in a 70% relative humidity-D_2O buffered environment at 23 °C. The sample used in the diffraction experiment was ground and packed under these conditions. The infrared spectrum of ilesite (Fig. 5) was obtained with a Nicolet Avatar 320 Fourier-transform infrared spectrometer and a Golden Gate diamond ATR. Comparison of the ilesite spectra with that of H_2O show there to be very little hydrogen in the sample studied.

Bianchite

Colorless goslarite crystals were crystallized from solution at room temperature with 10 g reagent grade $ZnSO_4$ (Fisher Z234Z) and 15 mL of 0.1 M D_2SO_4 prepared from D_2O (AECL ZX098)

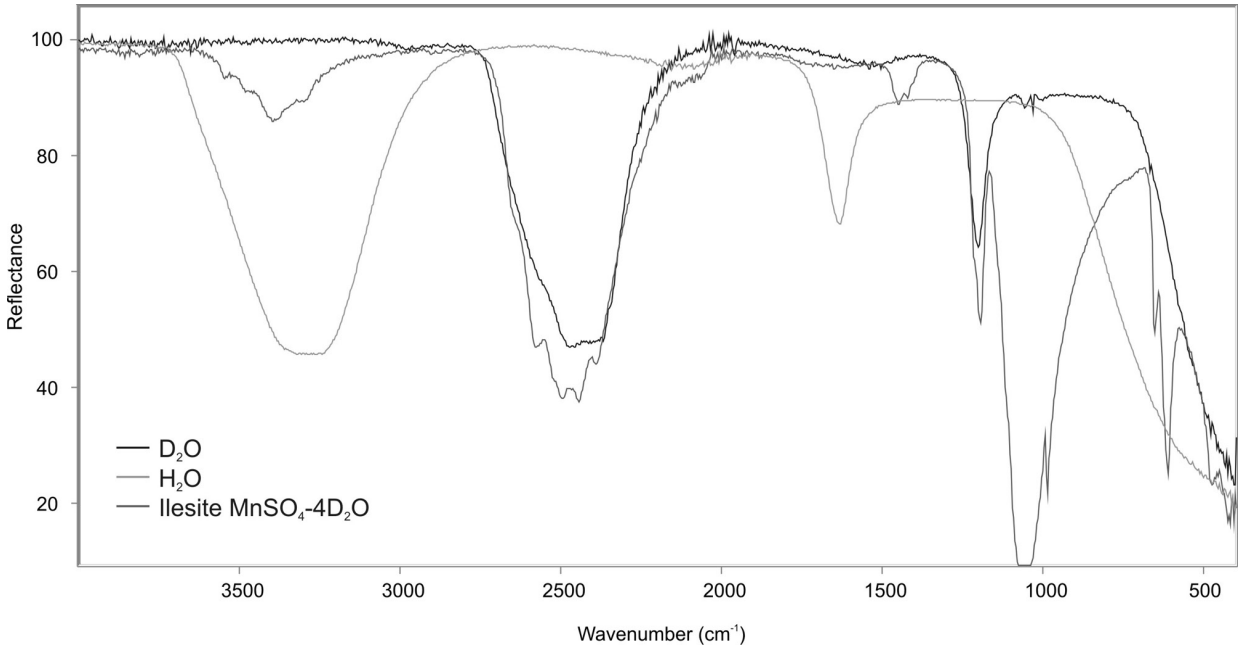

FIGURE 5. Infrared reflectance spectra of deuterated ilesite.

and D_2SO_4 (C/D/N Isotopes Inc. D-39). The deuterated goslarite was ground with a mortar and pestle within a chamber of 59% relative humidity (Anderson and Peterson 2005), buffered by a NaBr-D_2O saturated solution (Fisher S255 and AECL ZX098, respectively). The sample was ground periodically within the controlled-humidity environment to encourage complete dehydration to bianchite. The sample was confirmed as a single-phase bianchite by X-ray powder diffraction analysis prior to the neutron experiment. The infrared spectra for bianchite (Fig. 4) was obtained with a Nicolet Avatar 320 Fourier-transform infrared spectrometer and a Golden Gate diamond ATR.

Neutron diffracton experiments

The powdered samples were packed in a vanadium sample canister and sealed with soft malleable indium wire to prevent hydration or dehydration during the neutron experiment. Neutron diffraction data from powders of bianchite, boyleite, and ilesite were collected using wavelengths of 1.3308(1) and 2.3734(1) Å at room temperature using the Dualspec C2 high-resolution constant-wavelength powder diffractometer at the NRU reactor at Chalk River Laboratories [Canadian Neutron Beam Centre (CNBC), Chalk River, Ontario]. The neutron wavelengths were calibrated with the external standard NIST Si 640b. Neutron powder diffraction data were collected over a scattering range of 10 to 90 °2θ using a pyrolitic graphite filter and a silicon (311) monochromator at 92.7 °2θ.

The initial atom positions used in the boyleite refinement were taken from Blake et al. (2001) and those for ilesite were taken from Held and Bohaty (2002). Atomic structures were refined in the same unit-cell orientation as other rozenite group minerals to enable a convenient comparison with the isostructural phases (Table 1). The atomic structures were refined with the program GSAS (Larson and Von Dreele 2000) to R_{wp}(tot) 3.52% and R_p(tot) 2.48% for boyleite and R_{wp}(tot) 3.54% and R_p(tot) 2.51% for ilesite (Table 2). Neutron scattering lengths were taken from Sears (1992). No bond lengths or angles were restrained during the final least-squares cycles of the refinement. Atom coordinates and selected bond lengths and angles for boyleite and ilesite are presented in Tables 3 and 4, and hydrogen bonds for boyleite are represented schematically in Figure 6. CIFs available on deposit[1].

Table 2. Crystallographic data and refinement results for boyleite and ilesite, by combined histogram neutron powder diffraction refinement

	Boyleite	Ilesite
a (Å)	5.9144(2)	5.9753(1)
b (Å)	13.5665(4)	13.8186(3)
c (Å)	7.8924(2)	8.0461(1)
β°	90.688(2)	90.826(2)
V (Å³)	633.22(3)	664.31(2)
	Refinements	
Neutron λ (Å)	2.3734	2.3734
No. obs.	648	134
R_{wp}	3.78%	4.19%
R_p	2.26%	2.67%
Neutron λ (Å)	1.3308	1.3308
No. obs.	2035	1119
R_{wp}	3.36%	3.15%
R_p	2.6%	2.4%
Total R_{wp}	3.5%	3.5%
Total R_p	2.5%	2.5%

Note: Space group $P2_1/n$, $Z = 4$.

Table 3. Atom coordinates and equivalent isotropic-displacement parameters for boyleite ($ZnSO_4 \cdot 4D_2O$) and ilesite ($MnSO_4 \cdot 4D_2O$)

	Boyleite(Zn)				Ilesite(Mn)			
	x	*y*	*z*	U_{iso}	*x*	*y*	*z*	U_{iso}
M^{2+}	0.068(1)	0.1014(6)	0.219(1)	0.5(2)	0.066(2)	0.106(1)	0.210(2)	1.4(4)
S	0.191(3)	0.106(1)	0.828(2)	0.2(4)	0.195(3)	0.106(1)	0.823(2)	0.2(5)
O1	0.001(2)	0.0473(6)	0.756(1)	2.4(3)	0.008(2)	0.0512(7)	0.753(1)	2.5(3)
O2	0.250(2)	0.0761(7)	0.999(1)	2.0(3)	0.254(1)	0.0746(9)	0.992(1)	2.8(4)
O3	0.394(2)	0.0918(8)	0.718(1)	2.4(3)	0.392(2)	0.0967(9)	0.715(1)	2.5(3)
O4	0.130(2)	0.2116(7)	0.821(1)	2.3(3)	0.144(2)	0.2121(8)	0.820(1)	2.6(3)
Ow1	0.368(2)	0.0762(8)	0.357(2)	3.0(3)	0.375(2)	0.0739(9)	0.357(2)	3.3(4)
Ow2	0.778(2)	0.1406(8)	0.084(2)	2.2(3)	0.760(2)	0.1397(9)	0.088(2)	2.7(4)
Ow3	0.881(2)	0.1244(8)	0.444(1)	1.9(3)	0.884(2)	0.1281(9)	0.444(2)	2.7(3)
Ow4	0.180(2)	0.2484(7)	0.217(1)	1.3(2)	0.180(2)	0.2521(8)	0.221(1)	1.8(3)
D1a	0.364(2)	0.0850(9)	0.473(2)	3.9(4)	0.376(2)	0.086(1)	0.475(2)	6.1(5)
D1b	0.457(2)	0.0212(9)	0.326(2)	3.8(4)	0.466(2)	0.0189(9)	0.334(1)	3.0(3)
D2a	0.673(2)	0.1817(9)	0.144(2)	5.9(5)	0.665(2)	0.1906(9)	0.147(2)	6.1(4)
D2b	0.680(2)	0.091(1)	0.045(2)	6.5(5)	0.655(2)	0.096(1)	0.044(2)	7.0(5)
D3a	0.804(2)	0.185(1)	0.454(2)	4.7(5)	0.801(2)	0.1870(9)	0.461(2)	3.8(4)
D3b	0.920(2)	0.096(1)	0.547(2)	4.9(4)	0.912(2)	0.101(1)	0.550(2)	4.3(4)
D4a	0.310(2)	0.2658(8)	0.285(1)	2.9(4)	0.317(2)	0.267(8)	0.286(1)	3.8(4)
D4b	0.577(2)	0.1936(9)	0.728(2)	3.7(4)	0.589(2)	0.1910(8)	0.719(2)	3.8(4)

Notes: Neutron scattering from D positions was modeled using the scattering for D and a common site population for all positions was refined to determine the D:H ratio. Results of the refinement yield 91% D for boyleite and 95% D for ilesite.

The initial atomic positions for bianchite, including D positions, were taken from the structure of moorhouseite (Kellersohn et al. 1993a). The atomic structure was refined in a combination-histogram refinement using the two different wavelength measurements with the program GSAS (Larson and Von Dreele 2000). Neutron scattering lengths were taken from Sears (1992). The bonds of the sulfate tetrahedra were restrained to 1.44 ± 0.04 Å and the D-O bond lengths were restrained to 0.95 ± 0.07 Å. and the final restraint contribution was calculated using $[X^2_{(res)}/\text{no. obs}_{(res)}]/[X^2_{(tot)}/\text{no. obs}_{(tot)}] = 1.35\%$. The final least-squares cycle yielded $R_{wp(tot)} = 2.76\%$ and $R_{p(tot)} = 2.13\%$. Details of the refinement are listed in Table 5. Atomic coordinates, as determined by the combined histogram refinement, are listed in Table 6. All D sites were required to have the same occupancy and the final refined D site occupancy is x = 0.72(8). The scattering from this site is modeled as D_x and $\square_{1-x}$ (where $\square$ represents a vacancy in the scattering model). Assuming the sites are fully occupied with a D/H mixture and given the coherent neutron scattering lengths of D (6.67 fm) and H (–3.74 fm), the fractional occupancy may be recalculated to give $D_{0.86}H_{0.14}$ for all proton positions. Selected bond lengths and angles are presented in Table 7, and the hydrogen bonding is schematically represented in Figure 7.

Hydrogen bonding in rozenite group minerals

The hydrogen bonds observed in boyleite and ilesite specimens have been plotted in Figure 8 as well as hydrogen bond lengths taken from the literature for $M^{2+}SO_4 \cdot nH_2O$ sulfates (Chiari and Ferraris 1982). The bond lengths reported here for boyleite and ilesite are a significant improvement from the H-positions determined by previous X-ray diffraction studies (Blake

[1] Deposit item AM-12-076, CIFs. Deposit items are available two ways: For a paper copy contact the Business Office of the Mineralogical Society of America (see inside front cover of recent issue) for price information. For an electronic copy visit the MSA web site at http://www.minsocam.org, go to the *American Mineralogist* Contents, find the table of contents for the specific volume/issue wanted, and then click on the deposit link there.

TABLE 4a. Selected bond lengths (Å) and angles (°) for boyleite and ilesite as determine by the combined neutron diffraction refinements of their atomic structures

M-octahedra						Sulfate tetrahedra					
	Zn	Mn		Zn	Mn		Zn	Mn		Zn	Mn
M-O1	2.07(1)	2.24(2)	O1-M-O2	91.4(5)	91.1(7)	S-O1	1.48(2)	1.45(2)	O1-S-O2	110(1)	112(1)
M-Ow1	2.10(1)	2.22(2)	O1-M-Ow1	87.6(5)	84.2(7)	S-O2	1.46(2)	1.46(2)	O1-S-O3	110(1)	110(1)
M-Ow2	2.08(1)	2.12(2)	O1-M-Ow2	97.8(5)	96.0(7)	S-O3	1.50(2)	1.48(2)	O1-S-O4	109(1)	110(1)
M-Ow3	2.12(1)	2.21(2)	O1-M-Ow3	87.5(5)	85.4(6)	S-O4	1.48(2)	1.50(2)	O2-S-O3	110(1)	110(1)
M-Ow4	2.10(1)	2.13(2)	O2-M-Ow1	87.8(5)	87.4(7)	<S-O>	1.48(2)	1.47(2)	O2-S-O4	107(1)	111(2)
M-O2	2.08(1)	2.14(2)	O2-M-Ow2	92.8(6)	97.1(8)				O3-S-O4	111(1)	104(1)
<M-O>	2.09(1)	2.18(2)	O2-M-Ow4	89.0(5)	93.1(7)				<O-S-O>	109(1)	110(1)
			Ow1-M-Ow3	92.1(6)	89.4(7)						
			Ow1-M-Ow4	84.0(6)	84.5(7)						
			Ow2-M-Ow3	87.5(6)	86.1(7)						
			Ow2-M-Ow4	90.6(5)	94.6(8)						
			Ow3-M-Ow4	92.0(6)	89.7(7)						
			<Ow-M-Ow>	90.0(6)	89.9(7)						

Note: Mean values are reported in parentheses.

TABLE 4b. Hydrogen bond lengths (Å) and angles (°) for boyleite and ilesite

Water molecule	O···O	O···D-O	O···D	D-Ow	Ow-D	D···O	O···O	O···D-O	D-D	D-O-D
Boyleite										
O3···D1a-Ow1-D1b···O3		171(2)	1.95(1)	0.92(2)	0.95(1)	1.81(1)	174(2)		1.55(2)	112(2)
O4···D2a-Ow2-D2b···O2		146(2)	2.03(2)	0.96(2)	***0.94(2)***	***2.33(2)***	***3.02(2)***	***129(2)***	1.46(2)	100(2)
Ow2-D2b···O2					***0.94(2)***	***2.57(2)***	***3.31(2)***	***135(2)***		
O4···D3a-Ow3-D3b···O1	***2.84(2)***	***143(2)***	***2.03(2)***	***0.95(2)***	0.93(1)	1.84(2)	176(2)		1.56(2)	113(2)
Ow4···D3a-Ow3	***3.02(2)***	***123(2)***	***2.39(2)***	***0.95(2)***						
O4···D4a-Ow4-D4b···O3		154(2)	1.94(1)	0.96(1)	1.00(1)	1.94(1)	172(2)		1.54(2)	103(1)
<O···D-Ow-D···O>					0.95	2.01			1.53	107
Ilesite										
O3···D1a-Ow1-D1b···O3		174(2)	1.94(2)	0.96(2)	0.96(2)	1.86(1)		173(2)	1.56(2)	109(2)
O4···D2a-Ow2-D2b···O2		148(2)	1.94(2)	1.02(2)	***0.94(2)***	***2.44(2)***	***3.03(2)***	***121(2)***	1.56(2)	104(2)
Ow2-D2b···O2					***0.94(2)***	***2.43(2)***	***3.24(2)***	***142(2)***		
O4···D3a-Ow3-D3b···O1	***2.81(2)***	***138(2)***	***2.02(2)***	***0.96(2)***	0.94(2)	1.86(1)	2.79(2)	167(2)	1.53(1)	105(2)
Ow4···D3a-Ow3	***3.05(2)***	***126(2)***	***2.38(2)***	***0.96(2)***						
O4···D4a-Ow4-D4b···O3		***155(2)***	1.99(1)	0.98(1)	0.96(1)	1.76(1)		169(2)	1.54(2)	105(2)
<O···D-Ow-D···O>					0.97	2.02			1.55	106

Notes: Mean values are reported in parentheses. The values in bold and italics are the lengths of the bifurcated hydrogen.

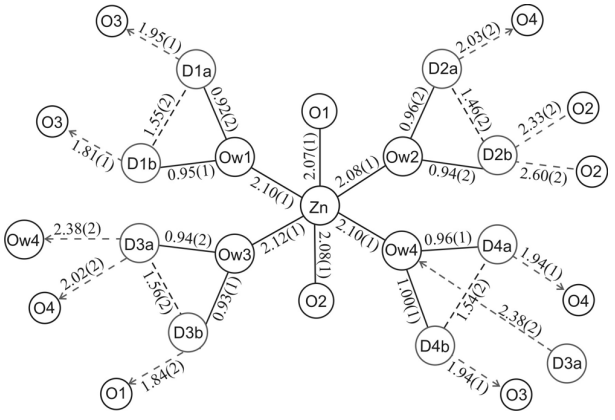

FIGURE 6. Schematic diagram of the bond network in boyleite, as determined by the combined histogram powder neutron diffraction refinement of the structure of deuterated boyleite $ZnSO_4{\cdot}4D_2O$. D···O distances (Å) are presented as dashed lines with arrows indicating the O-acceptor atom. Atoms D3a and D2b are considered to be involved in bifurcated hydrogen bonding.

et al. 2001; Held and Bohaty 2002) and now plot within the range of expected H-bonds from neutron diffraction studies of similar crystalline hydrates (Chiari and Ferraris 1982).

Previous interpretations of H-bonding in rozenite group minerals have concluded that one H-atom does not participate in H-bonding (H2b) (Baur 1964a; Blake et al. 2001). More recent interpretations have considered the hydrogen bond in question

TABLE 5. Crystallographic data and refinement results for bianchite by a combined histogram neutron powder diffraction least-squares refinement

a (Å)	9.969(1)
b (Å)	7.2441(7)
c (Å)	24.249(3)
β (°)	98.488(5)
V (Å^3)	1732.0(4)
neutron λ	2.3734Å
No. of obs. refl.	599
R_{wp}	2.73%
R_p	2.09%
neutron λ	1.3308Å
No. of obs. refl.	1157
R_{wp}	2.78%
R_p	2.16%
Total R_{wp}	2.76%
Total R_p	2.13%

Note: Space group *C2/c* and *Z* = 8.

is bifurcated between two acceptor O-atoms, resulting in long, weak hydrogen bonds (Kellersohn 1992; Held and Bohaty 2002). Based on a survey of water molecules (Chiari and Ferraris 1982) the longest acceptable H-bond between a donor H-atom and an acceptor O-atom is 2.258 Å, although the authors accept H···O distances associated with bifurcated bonds, as long as 2.948 Å. The "energy" of H-bonds (Brow, 1976) in crystalline hydrates studied by neutron diffraction is plotted as a curved line with H···O distances and O-H···O angles in Figure 9. The "energy" of an H···O bond is directly related to the density of O-acceptors. The hydrogen bonds in boyleite and ilesite, determined by neutron diffraction, are plotted against the energy curve and the

TABLE 6. Fractional atomic coordinates and isotropic displacement parameters for bianchite

	X	Y	Z	U_{iso}
Zn1	0	0	0	1.4(4)
Zn2	0	0.948(4)	0.25	1.4(4)
S	0.867(2)	0.455(2)	0.1258(7)	2.4(1)
O1	0.766(2)	0.594(2)	0.1325(7)	2.4(1)
O2	0.990(2)	0.447(3)	0.167(7)	2.4(7)
O3	0.910(2)	0.496(2)	0.0727(6)	2.4(1)
O4	0.802(2)	0.276(2)	0.1191(7)	2.4(1)
O5	0.594(2)	0.728(2)	0.0422(7)	2.4(1)
O6	0.543(2)	0.324(3)	0.0639(7)	2.4(1)
O7	0.316(2)	0.550(3)	0.0190(7)	2.4(1)
O8	0.878(2)	0.156(2)	0.2846(8)	2.4(1)
O9	0.894(2)	0.756(2)	0.2840(8)	2.4(1)
O10	0.861(2)	0.945(3)	0.1823(7)	2.4(1)
D51	0.156(2)	0.202(3)	0.0759(7)	5.5(2)
D52	0.043(2)	0.326(3)	0.0541(9)	5.5(2)
D61	0.011(3)	0.285(3)	0.930(1)	5.5(2)
D62	0.895(2)	0.173(3)	0.9038(8)	5.5(2)
D71	0.208(2)	0.874(2)	0.9530(7)	5.5(2)
D72	0.273(2)	0.973(3)	0.0042(9)	5.5(2)
D81	0.319(2)	0.609(3)	0.3103(9)	5.5(2)
D82	0.433(2)	0.758(3)	0.2959(9)	5.5(2)
D91	0.432(2)	0.141(3)	0.2988(9)	5.5(2)
D92	0.305(2)	0.226(3)	0.2696(8)	5.5(2)
D101	0.659(2)	0.344(3)	0.3433(9)	5.5(2)
D102	0.656(2)	0.553(3)	0.3407(8)	5.5(2)

Notes: All non-D sites are modeled as fully occupied. The site occupancy of all the D positions were constrained to be equal and refined to a value of 0.78(2) + 0.22 vacancy, which approximates the same scattering as $D_{0.86}H_{0.14}$ ($U_{iso}\times10^2$).

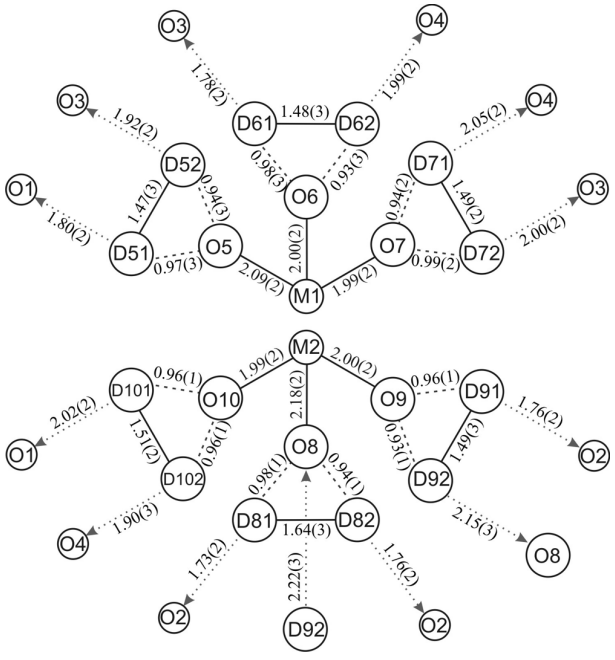

FIGURE 7. Schematic illustration of hydrogen bonding in bianchite. O8 is distinguished as it also acts as an acceptor from D92 and the M2-O8 bond is the longest Zn-O bond in the bianchite structure.

data compiled by Brown (1976). H···O bonds longer than 2.5 Å and with corresponding O-H···O angles <120° are too weak to be considered as a bonding interaction. However the bond length data for boyleite and ilesite in Figure 9 show a significant number of the hydrogen bonds that have acceptor bond lengths <2.5 Å and O-H···O angles of <150°. Bifurcated bonds identified by Brown (1976) and indicated as small triangles in Figure 9 also show a similar distribution of longer acceptor bond lengths and lower angles. The hydrogen bonding in boyleite and ilesite has a significant number of distorted hydrogen bonds because of the requirement that the groups of four-membered rings, shown in Figure 1, must be held together and packing consideration requires that some of these inter-cluster hydrogen linkages may not be optimal.

HYDROGEN BONDING IN BIANCHITE

The structure of the hexahydrite group of minerals ($M^{2+}SO_4{\cdot}6H_2O$; M^{2+} = Fe, Mg, Ni, Mn, Zn) varies very little between the different mineral species. The structure consists of two crystallographically unique M^{2+} sites (M1 and M2) that are coordinated by six water molecules. There is one crystallographically unique sulfate tetrahedron. The polyhedra of bianchite are linked via a three-dimensional network of hydrogen bonds formed between the hydrogen of the water molecules coordinating zinc and the oxygen atoms of the sulfate tetrahedra. The only exception is the hydrogen bond between D92 and O8 of the M2

TABLE 7. Selected bond lengths (Å) and angles (°) for bianchite as determined by the combined histogram neutron powder diffraction least-squares refinement

Zn1 octahedron		Zn2 octahedron		Sulfate tetrahedron							
Zn1-O5 ×2	2.09(2)	Zn2-O8 ×2	2.18(2)	S-O1	1.451(8)						
Zn1-O6 ×2	2.00(2)	Zn2-O9 ×2	2.00(2)	S-O2	1.456(8)						
Zn1-O7 ×2	1.99(2)	Zn2-O10 ×2	1.99(2)	S-O3	1.446(8)						
<Zn-O>	2.03		2.06	S-O4	1.447(8)						
				<S-O>	1.450						
O5-Zn1-O6	95.5(7)	O8-Zn2-O9	87.9(7)	O1-S-O2	118.6(2)						
O5-Zn1-O6	84.5(7)	O8-Zn2-O10	87.9(9)	O1-S-O3	104.9(1)						
O5-Zn1-O7	96.1(8)	O8-Zn2-O10	92.9(8)	O1-S-O4	109.1(2)						
O5-Zn1-O7	83.9(8)	O9-Zn2-O9	91.6(1)	O2-S-O3	106.4(2)						
O6-Zn1-O7	91.9(7)	O9-Zn2-O10	89.2(1)	O2-S-O4	111.1(2)						
O6-Zn1-O7	88.1(7)	O9-Zn2-O10	90.0(1)	O3-S-O4	105.8(2)						
mean	90.0	mean	90.2	mean	109.3						
				Hydrogen bonding							
Water molecule	O···O	O···D-O	O···D	D-Ow	Ow-D	D···O	O···D-O	O···O	D-D	D-O-D	
O1...D51-O5-D52···O3	2.75	165	1.80(2)	0.97(1)	0.94(1)	1.92(2)	169	2.85	1.47(3)	101.1(3)	
O3···D61-O6-D62···O4	2.74	169	1.78(2)	0.98(1)	0.93(1)	1.99(2)	138	2.75	1.48(3)	101.6(3)	
O4···D71-O7-D72···O3	2.49	161	2.05(2)	0.94(1)	0.99(1)	2.00(2)	159	2.94	1.49(2)	101.9(2)	
O1···D81-O8-D82···O2	2.67	160	1.73(2)	0.98(1)	0.94(1)	1.76(2)	163	2.67	1.64(3)	118.1(3)	
O2···D91-O9-D92···O8	2.72	172	1.76(2)	0.96(1)	0.93(1)	2.15(3)	164	3.05	1.49(3)	103.7(3)	
O1···D101 O10 D102···O4	2.92	155	2.02(2)	0.96(1)	0.96(1)	1.90(3)	174	2.86	1.51(2)	103.4(2)	
mean	2.72	164	1.86	0.97	0.95	1.95	161	2.85	1.51	105	

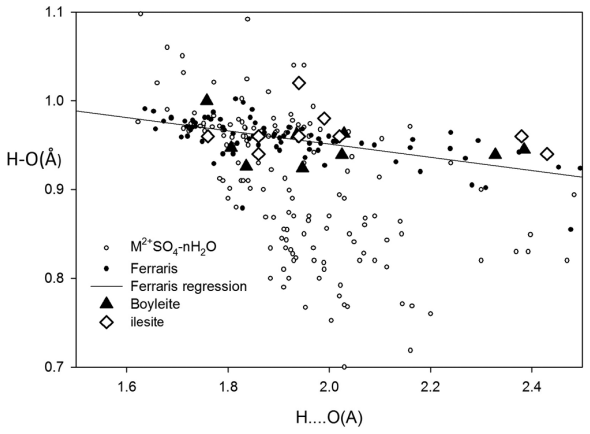

FIGURE 8. Water molecule H-O and H-bond distances. Small gray circles represent data bonds lengths for $M^{2+}SO_4 \cdot nH_2O$ minerals from the following papers: Angel and Finger (1988), Bacon and Titterton (1975), Bargouth and Will (1981), Baur and Rolin (1972), Baur (1964a, 1964b), Calleri et al. (1984), Elerman (1988), Gerkin et al. (1988), Hawthorne et al. (1987), Iskhakova et al. (1991), Kellersohn (1992), Kellersohn et al. (1993a, 1993b), Ptasiewicz-Bak et al. (1993), Wildner and Giester (1991), Zahrobsky and Baur (1965), Zalkin et al. (1964). Small black circles represent the bond lengths of crystalline hydrates studied by neutron diffraction [cited in Chiari and Ferraris (1982)]. The regression lines for these neutron data sets are presented as a solid line. The H-bonds for boyleite and ilesite determined by this study fall close to the line determined by Ferraris based on structures studied using neutron diffraction. The positions of the hydrogen atoms determined by neutron diffraction in the present study are a better estimate than those previously determined for the same minerals by X-ray diffraction analysis (Blake et al. 2001; Held and Bohaty 2002).

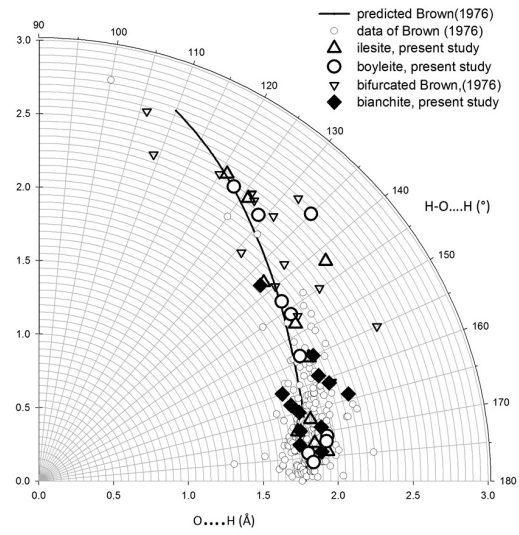

FIGURE 9. Hydrogen bond geometry after Brown (1976). The coordinates are H···O length and O-H···O angle. All of the hydrogen acceptor bonds in bianchite are <2.1 and make O-H···O angles close to 180° because the octahedra and tetrahedra within the structure are only held together by hydrogen bonding and are arranged to maximize hydrogen bond interactions. Ilesite and bianchite show a much larger range of acceptor bond length and O-H···O angle because the octahedra and tetrahedra are linked to form four-membered rings and the efficient packing of these rings requires some compromise in the hydrogen bonding and some hydrogen bonds to be bifurcated. H-bonds closest to the curve of predicted H-bond values are most reasonable and H-bonds longer than 2.5 Å with O-H···O angles <120° are not considered significant bonding interactions within a structure.

octahedron. The result of this hydrogen bonding is a lengthening of the M2-O8 bond resulting in a greater distortion of the M2 octahedron than the M1 octahedron (Kellersohn et al. 1993a; Angel and Finger 1988). The M2-O8 bond is the longest M-O bond in each of the hexahydrite group minerals. Figure 10 shows the linkage of hydrogen bonds that link the ZnO_6 together. The water molecule D81-O8-D82 has each D forming a bond with a sulfate oxygen but O8 also forms a hydrogen bond with D92 that is part of the adjacent ZnO_6 octahedron. Similar octahedral distortions, due to the lengthening of an M-O bond involved with addition hydrogen bond interaction, have been observed in minerals of the epsomite and melanterite groups (Anderson et

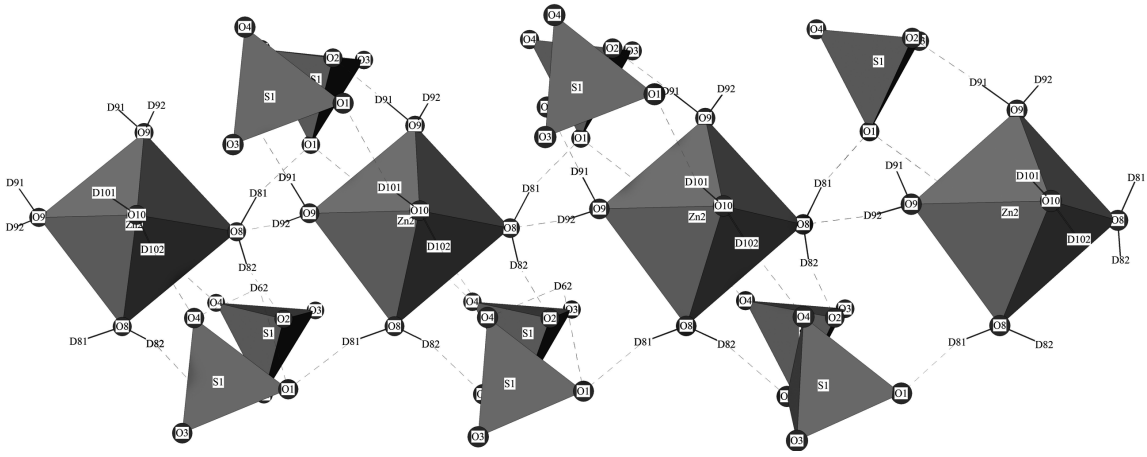

FIGURE 10. Hydrogen bonding in bianchite. The Zn2-O8 bond is the longest Zn-O bond in the structure (Table 7). Ow8 is bonded to two D atoms at 0.98 and 0.94 Å and these are each bonded to an oxygen of a sulfate tetrahedron. O8 also acts as an acceptor for a hydrogen bond from O9 through D92 (2.15 Å). No other oxygen atom in the structure has this extra hydrogen bond and this explains the longer length of the Zn-O8 bond.

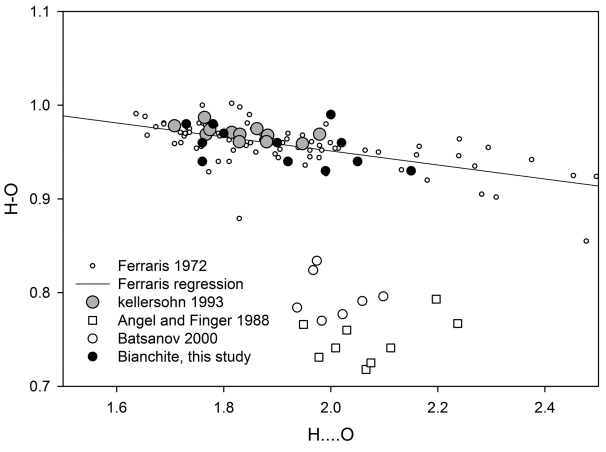

FIGURE 11. Plot of water molecule H-O distances and H-bond distances for hexahydrite group minerals. Bianchite bond lengths of this study are represented by solid black circles. Solid gray circles represent data from the moorhouseite single-crystal neutron diffraction electron density study (Kellersohn et al. 1993a). Open squares and solid triangles represent bond lengths as determined by X-ray diffraction studies for hexahydrite (Batsanov 2000) and Ni-hexahydrite (Angel and Finger 1988). These bonds are shorter that than those determined by neutron experiments because of the inaccurate biased hydrogen positions determined by X-ray diffraction analysis. The solid line is the linear regression of neutron determined data (small dots) compiled by the survey of H-bonds by Ferraris and Marchini-Angelo (1972).

al. 2005; Anderson and Peterson 2007). The hydrogen positions in Ni-hexahydrite (Angel and Finger 1988; Gerkin and Reppart 1988) and hexahydrite (Batsanov 2000; Zalkin et al. 1964) were determined by X-ray diffraction studies and report H-O distances shorter than those of deuterated moorhouseite (Kellersohn et al. 1993a) and the results for bianchite that are presented here. Acceptor hydrogen bonds in hexahydrite group minerals range from 1.7 to 2.1 Å (Fig. 11) and fall within the range of hydrogen bonds observed by Ferraris and Marchini-Angelo (1972).

ACKNOWLEDGMENTS

Thank you to A. Murray of the Department of Arts Conservation at Queen's University for the use of the Nicolet ATR-IR spectrometer. Lachlan Cranswick (NPMR/NRC) provided generous support of this project. An NSERC discovery grant to R.C.P. funded the research.

REFERENCES CITED

Anderson, J.L. and Peterson, R.C. (2005) Determination of sulfate mineral phase equilibria as a function of relative humidity. Intermediate compositions in the (Mg,Fe,Zn)$SO_4 \cdot H_2O$ system at 22 °C. Geological Association of Canada–Mineralogical Association of Canada, Program Abstracts, 30, 4.

——— (2007) The atomic structure and hydrogen bonding of deuterated melanterite $FeSO_4 \cdot 7D_2O$. Canadian Mineralogist, 45, 457–469.

Anderson, J.L., Peterson, R.C., and Swainson, I.P. (2005) Combined neutron powder and X-ray single-crystal diffraction refinement of the atomic structure and hydrogen bonding of goslarite ($ZnSO_4 \cdot 7H_2O$). Mineralogical Magazine, 69, 259–271.

Angel, R.J. and Finger, L.W. (1988) Polymorphism of nickel sulfate hexahydrate. Acta Crystallographica, C, 44, 1869–1873.

Ashley, P.M. and Lottermoser, B.G. (1999) Arsenic contamination at the Mole River mine, northern New South Wales. Australian Journal of Earth Sciences, 46, 861–874.

Bacon, G.E. and Titterton, D.H. (1975) Neutron diffraction studies of $CuSO_4 \cdot 5H_2O$ und $CuSO_4 \cdot 5D_2O$. Zeitschrift fürKristallographie, 141, 330–341.

Bakos, F., Carcanhiu, G., Fadda, S., Mazzella, A., and Valera, R. (1990) The gold mineralization of Baccu Locci (Sardinia, Italy); Origin, evolution and concentration processes in the geological diversity of gold. Terra Nova, 2, 234–239.

Bargouth, M.O. and Will, G. (1981) A neutron diffraction refinement of the crystal structure of tetragonal nickel sulfate hexahydrate. International Centre for Theoretical Physics: Report, Trieste, Italy.

Batsanov, A.S. (2000) Magnesium sulfate hexahydrate at 120K. Acta Crystallographica C, 56, e230–e231.

Baur, W.H. (1962) Zur Kristallchemie der Salzhydrate. Die Kristallstukturen von $MgSO_4 \cdot 4H_2O$ (Leonhardtit) und $FeSO_4 \cdot 4H_2O$ (Rozenit). Acta Crystallographica, 15, 815–826.

——— (1964a) On the crystal chemistry of salt hydrates. II. A neutron diffraction study of $MgSO_4 \cdot 4H_2O$. Acta Crystallographica, 17, 863–869.

——— (1964b) On the crystal chemistry of salt hydrates. III. The determination of the crystal structure of $FeSO_4 \cdot 7H_2O$ (melanterite). Acta Crystallographica, 17, 1167–1174.

——— (2002) Zinc(II) sulfate tetrahydrate and magnesium sulfate tetrahydrate. Addendum. Acta Crystallographica E, 58, e9–e10.

Baur, W.H. and Rolin, J.L. (1972) Salt hydrates. IX. The comparison of the crystal structure of magnesium sulfate pentahydrate with copper sulfate pentahydrate and magnesium chromate pentahydrate. Acta Crystallographica B, 28, 1448–1455.

Blake, A., Cooke, P., Hubberstey, P., and Sampson, C. (2001) Zinc(II) sulphate tetrahydrate. Acta Crystallographica E, 57, i109–i111.

Brown, I.D. (1976) On the geometry of O-H···O hydrogen bonds. Acta Crystallographica A, 32, 24–31.

Calleri, M., Gavetti, A., Ivaldi, G., and Rubbo, M. (1984) Synthetic epsomite, $MgSO_4 \cdot 7H_2O$: Absolute configuration and surface features of the complementary (111) forms. Acta Crystallographica, B, 40, 218–222.

Chiari, G. and Ferraris, G. (1982) The water molecule in crystalline hydrates studied by neutron diffraction. Acta Crystallographica B, 38, 2331–2341.

Chou, I-M. and Seal, R.R. II (2005) Determination of goslarite-bianchite equilibria by the humidity-buffer technique at 0.1 MPa. Chemical Geology, 215, 517–523.

Chou, I-M., Seal, R.R. II, and Hemingway, B.S. (2002) Determination of melanterite-rozenite and chalcanthite-bonattite equilibria by humidity measurements at 0.1 MPa. American Mineralogist, 87, 108–114.

Chou, I-M., Seal, R.R. II, and Piatack, N. (2005) Determination of hexahydrite-starkeyite equilibria by the humidity-buffer technique at 0.1 MPA: Implications for the Martian H_2O cycle. Salt Lake City annual meeting (Oct. 16–19, 2005) Geological Society of America abstracts with programs, 37, 5.

Dowty, E. (2011) ATOMS version 6.4. Shape Software, 521 Hidden Valley Road, Kingsport, Tennessee 37663, U.S.A. http://www. shapesoftware.com/.

Elerman, Y. (1988) Refinement of the crystal structure of $CoSO_4 \cdot 6H_2O$. Acta Crystallographica, C, 44, 599–601.

Ferraris, G. and Marchini-Angelo, M. (1972) Survey of the geometry and environment of water molecules in crystalline hydrates studied by neutron diffraction. Acta Crystallographica, 28, 3572–3583.

Gaines, R.V., Skinner, H.C.W., Foord, E.E., Mason, B., and Rosenzweig, A. (1997) Dana's New Mineralogy (8th ed.). Wiley, New York.

Gerkin, R.E. and Reppart, W.J. (1988) Structure of monoclinic nickel(II) sulphate hexahydrate. Acta Crystallographica C, 44, 1486–1488.

Greenspan, L. (1977) Humidity fixed points of binary saturated aqueous solutions. Journal of Research of the National Bureau of Standards-A. Physics and Chemistry, 81A, 89–96.

Grevel, K. and Majzlan, J. (2009) Internally consistent thermodynamic data for magnesium sulfate hydrates. Geochimica et Cosmochimica Acta, 73, 6805–6815.

Guenot, J., Manoli, J.-M., and Bregeault, J.-M. (1969) Thermogravimétrie des systèmes solides-gaz. Déshydratation thermique des sulfates de cobalt et de zinc hydratés. Bulletin de la Société Chimique de France, 8, 2666–2670.

Hawthorne, F.C., Groat, L.A., Raudsepp M., and Ercit T.S. (1987) Kieserite, $Mg(SO_4) \cdot (H_2O)$, a titanite group mineral. Neues Jahrbuch für Mineralogie Abhandlungen, 157, 121-132.

Held, P. and Bohaty, L. (2002) Manganese(II) sulfate tetrahydrate (ilesite). Acta Crystallographica, E, 58, i121–i123.

Iskhakova, L.D., Dubrovinskii, L.S., and Charushnikova, I.A. (1991) Crystal structure, calculation of parameters of atomic interaction potential and thermochemical properties of $NiSO_4 \cdot nH2O$ (n=7,6). Zeitschrift für Kristallographie, 36, 650–655.

Jambor, J.L. and Boyle, R.W. (1962) Gunningite, a new zinc sulphate from the Keno Hill-Galena Hill area, Yukon. Canadian Mineralogist, 7, 209–218.

——— (1965) Moorhouseite and aplowite, new cobalt minerals from Walton, Nova Scotia. Canadian Mineralogist, 8, 166–171.

Jambor, J.L. and Traill, R.L. (1963) On rozenite and siderotil. Canadian Mineralogist, 7, 751–763.

Kellersohn, T. (1992) Structure of cobalt sulfate tetrahydrate. Acta Crystallographica, C, 48, 776–779.

Kellersohn, T., Delaplane, R.G., and Olovsson, I. (1993a) The experimental electron density in monoclinic cobalt sulfate hexahydrate, $CoSO_4 \cdot 6D_2O$ at 25K. Acta

Crystallographica, B, 49, 179–192.
——— (1993b) Disorder of a trigonally planar coordinated water molecule in cobalt sulfate heptahydrate, $CoSO_4 \cdot 7D_2O$ (bieberite). Zeitschrift für Naturforschung, 46, 1635-1640.9.
Larsen, E.S. and Glenn, M.L. (1920) Some minerals of the melanterite and chalcanthite groups with optical data on the hydrous sulphates of manganese and cobalt. American Journal of Science, 50, 225–233.
Larson, A.C. and Von Dreele, R.B. (2000) General Structure Analysis System (GSAS). Los Alamos National Laboratory Report LAUR 86-748.
Pannetier, G., Bregeault, J.-M., and Tardy, M. (1966) Etude de la dissociation thermique des sulfates et des sulfates basiques. VI. Mise en evidence et étude cristallographique du sulfate de zinc tetrahydrate $ZnSO_4 \cdot 4H_2O$. Memoires Présentés à la Société Chimique, 55, 324–326.
Pasava, J., Breiter, K., Huka, M., and Korecky, J. (1986) Chavleticeite, $(Mn,Mg)SO_4 \cdot 6H_2O$, a new mineral. Neues Jahrbuch für Mineralogie Monatshefte, 121–125.
Perroud, P., Meisser, N., and Sarp, H. (1987) Présence de zincocopiapite en Valais. Schweizerische Mineralogische und Petrographische Mitteilungen, 67, 115–117.
Peterson, R.C. and Grant, A. (2005) Dehydration and crystallization reactions of secondary sulfate minerals found in mine waste: *in situ* powder diffraction experiments. Canadian Mineralogist, 43, 1171–1181.
Ptasiewicz-Bak, H., Olovsson, I., and McIntyre, G.J. (1993) Bonding deformation and superposition in the electron density of tetragonal $NiSO_4 \cdot 6H_2O$ at 25K. Acta Crystallographica, B, 49, 192–201.
Rhomer, R. (1939) Dehydration of manganous sulfate heptahydrate by the aqueous method. Comptes Rendus, 209, 315–317.
Schuiling, R.D. (1992) Goslarite: threat or promise for the environment of the Geul Valley? Journal of Geochemical Exploration, 42, 383–386.
Sears, V. (1992) Neutron Scattering lengths and cross sections, Neutron News, 3, 29–37.
Sinha, S.G. and Deshpande N.D. (1989) Dehydration of crystalline $CoSO_4 \cdot 7H_2O$. Thermochimica Acta, 156, 1–10.
Uvaliev, Y.K. and Motornaya, G.A. (1989) Study of equilibrium dehydration pressure of zinc sulfate crystal hydrates. Izvestiya Akademii Nauk Kazakhskoi SSR, Seriya Khimicheskaya, 6, 54–57.
Vlasov, V.V. and Kuznetsov, A.V. (1962) Melanterite and the product of its alteration. Zapiski Vses Mineralog. Obshch, 91, 490–492.
Wagman, D.D., Evans, W.H., Parker, V.B., Schumm, R.H., Halow, I., Bailey, S.M., Churney, K.L., and Nuttal, R.L. (1982) The NBS tables of chemical thermodynamic properties. Selected values for inorganic and C1 and C2 organic substances in SI units. Journal of Physical Chemistry Reference Data, 11, 392.
Walenta, K. (1978) Boyleite, a new sulphate mineral from Kropback, Southern Black Forest. Chemie der Erde, 37, 73–79. (In Fleischer, M., Chao, G., and Pabst, A. (1979) New Mineral Names, American Mineralogist, 64, 241–245.)
Wildner, M. and Giester, G. (1991) The crystal structures of kieserite-type compounds. I. Crystal structures of $Me(II)SO_4 \cdot H_2O$ (Me = Mn, Fe, Co, Ni, Zn). Neus Jahrbuch für Mineralogie, 7, 296–306.
Zahrobsky, R.F. and Baur, W.H. (1965) The crystal structure of copper(II) sulfate trihydrate. Naturwissenschaften, 52, 389–389.
Zalkin, A., Ruben, H., and Templeton, D.H. (1964) The crystal structure and hydrogen bonding of magnesium sulfate hexahydrate. Acta Crystallographica, 17, 235–240.

Manuscript received February 1, 2012
Manuscript accepted July 3, 2012
Manuscript handled by Simon Redfern